



Article

Influence of Concentration of Sodium Metasilicate and Descaling on the High Temperature Lubricating Effects Evaluated by Hot Rolling Mill

Hongliang Liu ¹, Xun Wu ¹, Jiaxuan Huang ¹, Xibo Shao ¹, Pei Wang ², Guanyu Deng ^{3,*} and Long Wang ^{1,*}

¹ State Key Laboratory of Solidification Processing, Center of Advanced Lubrication and Seal Materials, Northwestern Polytechnical University, Xi'an 710072, China; mayoi@mail.edu.cn (H.L.)

² School of Materials Science and Engineering, Henan University of Technology, Zhengzhou 450001, China

³ Faculty of Engineering and Information Sciences, University of Wollongong, Northfields Avenue, Wollongong, NSW 2522, Australia

* Correspondence: gdeng@uow.edu.au (G.D.); longw@nwpu.edu.cn (L.W.)

Abstract: Lubricant is vital to improve energy efficiency and workpiece durability for the moving counterpart. High-temperature lubricants are important for the hot rolling process to reduce the rolling force and protect the roller and the strips. The current paper concerns eco-friendly sodium metasilicate as a high-temperature lubricant. A hot rolling mill is employed to evaluate the lubrication effect of sodium metasilicate. The influence of crucial factors of concentration of lubricant and descaling is discussed; the rolled surface was analyzed by scanning electron microscopy, energy dispersive spectroscopy, and 3D profilometer. The results depict that the sodium metasilicate can reduce the rolling force by about 7.8% when the concentration of sodium metasilicate is 18% and above, and descaling of the hot stripe makes the lubrication effect more effective, which can reach a 12.7% reduction in the rolling force. This lubrication is attributed to the formed melts of the sodium silicate layer that offers an easy shearing interface. For the un-descaled samples, the lubricant will be compacted and mixed with the oxide scale, and weakens the lubrication effect. This work suggests that sodium metasilicate can be a high-temperature lubricant for hot rolling; descaling is vital, not only for the quality of the product but also for the efficiency of the lubricant. This work will also be useful for the concentration selection of glass lubricant.



Citation: Liu, H.; Wu, X.; Huang, J.; Shao, X.; Wang, P.; Deng, G.; Wang, L. Influence of Concentration of Sodium Metasilicate and Descaling on the High Temperature Lubricating Effects Evaluated by Hot Rolling Mill. *Lubricants* **2023**, *11*, 352. <https://doi.org/10.3390/lubricants11080352>

Received: 6 July 2023

Revised: 5 August 2023

Accepted: 15 August 2023

Published: 18 August 2023



Copyright: © 2023 by the authors. Licensee MDPI, Basel, Switzerland. This article is an open access article distributed under the terms and conditions of the Creative Commons Attribution (CC BY) license (<https://creativecommons.org/licenses/by/4.0/>).

Keywords: high-temperature lubricant; hot rolling; sodium metasilicate

1. Introduction

Lubrication is crucial to make the key machinery contact components operate durably and reliably at extremely high temperatures, like the blade in the engine, the roller in the hot rolling process, etc. [1–6]. For hot metal forming processes, like hot rolling, the roller and work rolls are often exposed to high load (41 GPa) and elevated temperature (600–1200 °C) [7], leading to high friction, severe wear, oxidation, and thermal fatigue, etc., which will influence the quality of the product, the service life of the roller and the energy needed for deforming [8–14]. It is reported that effective lubricant can help solve these problems to improve the roll life (20% to 40%) and strip surface quality, as well as reduce power consumption [15,16].

Traditionally, an oil-in-water emulsion is used as a lubricant for hot rolling [17]. The oil is either Karanja ester and mineral oil [18–21]. Oil droplets are believed to enter the voids between contact asperities and function as friction-reducing and cooling agents, and several works also focus on the lubricating state using either experimental or simulation for the rolling process [22,23]. However, vulnerability to thermal degradation is speculated to undermine the performance of hydrocarbon-based lubricants. Additionally, the oil-based, grease-based lubricants can only perform effectively below 300 °C [24,25]. At high

temperatures, some solid lubricants, like layered graphite, h-BN, and nanoparticles, are normally used [26–28]. Further, melt (glass) lubricants exhibiting desirable physical and chemical properties are regarded as promising lubricants for hot metal forming.

The development of new, environmentally tribological systems has become an urgent demand due to growing environmental and energy concerns, particularly to substitute the environmentally hazardous lubricants in the hot metal forming process [29]. Since 2000, hazardous lubricants in industrial applications have been increasingly restricted in Japan and Europe. EU has introduced new legislation for high-level protection of human health and the environment. Therefore, metal manufacturers are increasingly concerned about environmental pollution and have attempted to establish healthy and safe working conditions. In the hot metal forming, the graphite regarded as “black” lubricants needs to be replaced by the “white” lubricants due to the dirty working environment, pipe corrosion, leakage to the soil as well as the low recovery rate of inferior oil separation [30]. Water-based lubricant for metal forming has attracted increased attention due to their promising cooling effect and low environmental pollution [31,32].

Melt (glass), like silicates, borates, and phosphates, with the atomic structure of short-range order, while long-range out-of-order, are believed to be high-temperature lubricants. Borate-based compounds have been used as an additive in various lubricant formulations [33]. It can react with ferrous surfaces to form a coating that resists corrosion. Inorganic borates are oil additives that adapt to boundary lubricating conditions [34]. Borate additives have been applied in the metalworking industry, such as wire drawing and seamless tube production. However, not all of these melts obtain the lubrication effect. For example, the application of borate of soda alone or in a mixture of oil has caused a gumming up and a shut-down of the process in the production of seamless tubes.

The tribological effects of glass lubricant were mainly studied using a laboratory ball-on-disc tribometer. The mechanism of glass lubricant was discussed by surface and interface analysis. Tieu et al. [35,36] have studied the tribo-film of poly-phosphate, and indicate that molten poly-phosphate lubricant shows excellent properties in friction reduction, anti-wear, and anti-oxidation properties because of the tribo-induced hierarchical structure at the rubbing interface. They suggest that liquid-like melt forms a viscous lubrication film with Fe, Na, K, P, and O, providing reduced friction, wear, and anti-oxidation. The reactant film can relieve the stress concentration arising from the plastic deformation after sliding; an intermediate phosphate layer restricts free access of oxygen to the underlying surface and reduces secondary oxide scaling. Cui et al. [37,38] suggest that different chain lengths of poly-phosphate show a gradient change in composition on the tribo-interface. Liquid-like melt forms a viscous lubrication film, offering lubrication and anti-oxidation. The reactant film with Fe, Na, K, P, and O can relieve the local stress concentration during sliding; an intermediate phosphate layer restricts free access of oxygen to the underlying surface. The short-chain phosphate with lower viscosity on the top surface contributes to better lubrication and anti-wear efficiency. The long chain poly-phosphate adheres to iron oxide through a short-chain phosphate due to the tribochemical reaction between wear debris and phosphate agents. The interaction between $\text{Na}_4\text{P}_2\text{O}_7$ and Fe_2O_3 results in a mixed Na/Fe phosphate compound with a P-O-Fe bond, which replaces the P-O-P bond. In the meantime, iron oxide is digested by phosphate to make the poly-phosphate more cross-linking and improve the tribological properties [39]. Kong et al. [40] demonstrate that the mixture of sodium poly-phosphate and potassium poly-phosphate also shows excellent lubrication effects because of the multi-layers at the sliding interface.

As one of the glasses, sodium metasilicate is eco-friendly and is always used as a viscosity additive with other lubricants. Silicate-based compounds have been developed as lubricant additives, which minimize friction and wear effectively, e.g., $\text{Al}_4[\text{Si}_4\text{O}_{10}](\text{OH})_4$ [41], and aluminum–magnesium silicate [42]. Some publications mentioned about silicate additives in mineral oil [41–43]. Devendra Singh et al. [44] report that engine lubricant in a very low concentration of 0.01% weight/volume can reduce friction coefficient (46%) and wear scar diameter because of the presence of the ferrosilicate layer on tribosurfaces, which help

reduce friction and wear. Yu et al. [45] studied the serpentine mineral powders (1.5 wt.%, 1 μm in size) as lubricant additive in mineral oil and found that a nanocrystalline tribofilm with a thickness of 500–600 nm was generated on worn surface, mainly composed of Fe_3O_4 , FeSi , SiO_2 , AlFe and Fe-C compounds (Fe_3C). Feng Nan et al. [42] report that FeOOH and SiO formed on the worn surface after lubricating with ultrafine magnesium aluminum silicate powders as lubricant additives in oil is responsible for the further improvement in tribological properties. However, as the base of these lubricants, the lubrication of the NSO is merely studied, especially at high temperatures.

Little research concerns the lubrication effect of sodium metasilicate with other lubricants by simulated hot rolling mill. Although many patents [46] mentioned sodium silicate as a high-temperature lubricant, only a few papers [47] studied the combined sodium silicate (ratio of $\text{SiO}_2/\text{Na}_2\text{O}$ between 2 to 4) and graphite as a high-temperature lubricant from 500 to 1200 $^\circ\text{C}$ and found that the friction is lowest when the silicate is in the liquid state, and that graphite plays an important role for the adhesion. In hot metal forming, an oxide scale forms on the strips, and the influence of oxide and lubricant on rolling results is still unclear; the concentration is dependent on tribological results using pure sodium metasilicate lubricant and is rarely reported.

Therefore, in this work, the lubrication of NSO with varying concentrations (0, 3, 9, 18, 36, 54 wt.%) was used for the hot rolling process. The effect of descaling on the lubrication was also investigated. Surface and interface analyses were also conducted to identify the lubrication mechanism.

2. Materials and Methods

2.1. Materials

Sodium metasilicate (NSO) from Sigma–Aldrich was used as a lubricant for the hot rolling process. The X-ray diffraction (XRD) pattern of NSO is shown in Figure 1a. The NSO is a polymer's structure linked through the covalent repeated tetrahedral SiO_4 atoms to form chains and surrounded by Na, as shown in Figure 1b.

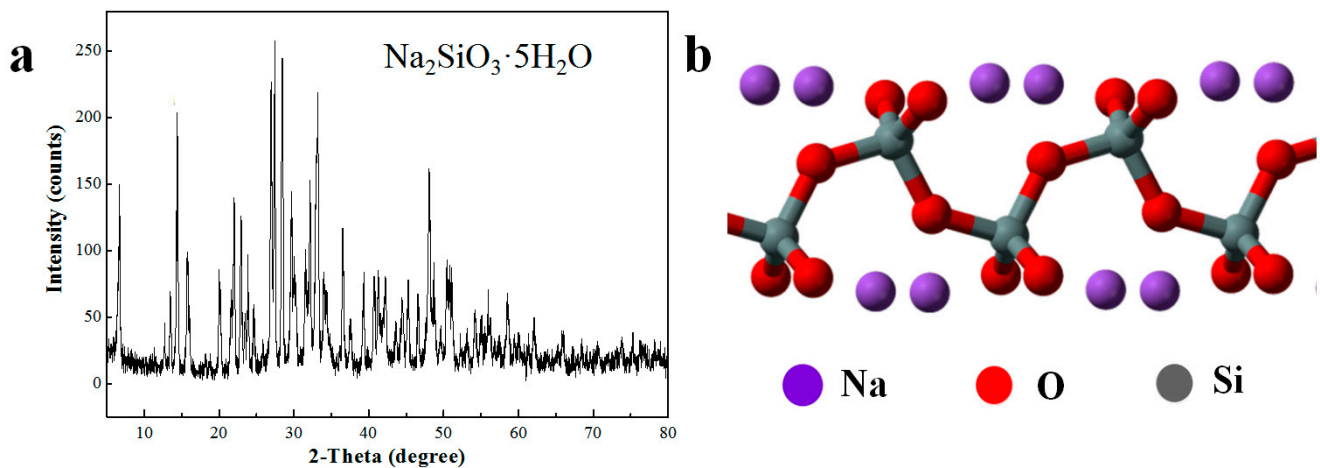


Figure 1. (a) XRD pattern of commercial sodium metasilicate, and (b) the structure of sodium metasilicate.

The commonly used mild steel (MS) plates were used for the hot rolling tests. The specimens were cut into 30 mm \times 20 mm \times 203 mm and chamfered at the front end. The composition of this MS is shown in Table 1. Nomenclature table with SI unit is shown in Table 2.

Table 1. Chemical composition of mild steel (%).

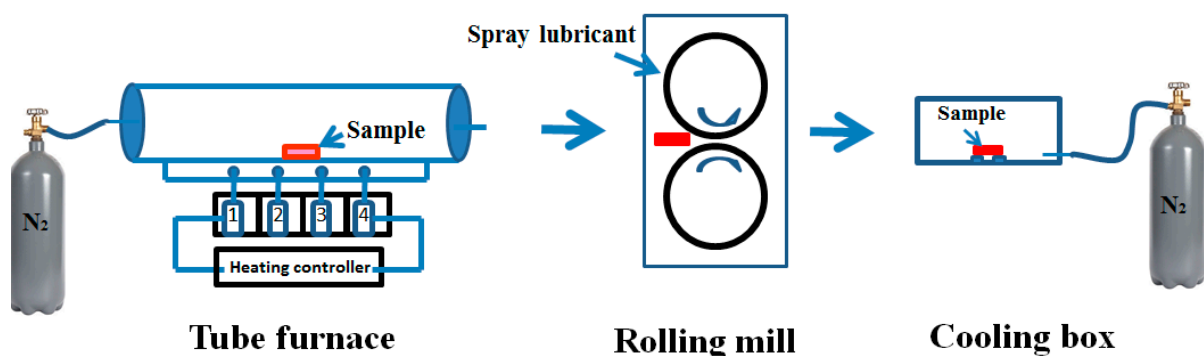
Elemrnt	Fe	C	Si	Mn	W	Al	Cu	P	S
content	98.17	0.5502	0.1626	0.8383	0.1008	0.00241	0.0038	0.0231	0.0516

Table 2. Nomenclature table with SI unit.

Name	Symbol	SI Units
Sodium metasilicate	NSO	
Mild steel	MS	
Roughness	Ra	μm
Rolling force	P	N
Coefficient of friction	μ	
Strip width	B	m
Radius of roll	R1	
Rolling reduction	Δh	
Front tension stress	t1	Pa
Back tension stress	t2	Pa
Yield stress	σ	Pa
Base yield stress	σ_0	Pa
Temperature	T	K
Stain	ε	
Stain rate	$\dot{\varepsilon}$	s^{-1}

2.2. Hot Rolling Experiment

The hot rolling experiments were conducted using a 2-high Hille 100 rolling mill. The roll size is 225 mm in diameter, 254 mm in length, and a roughness (R_a) of 1.0 μm . Rolling forces were obtained by load cells on the mill connected to a computer. The rolling torque was obtained using strain gauges on the shaft. Firstly, the MS sample was heated in a MoSi_2 tube heating furnace at 1150 $^\circ\text{C}$ for 30 min with the N_2 gas at a flow rate of 15 L/min to ensure a homogeneous temperature distribution and a uniform scale thickness. Then, it was rolled with a reduction of 40% (average pressure 132 MPa) and a rolling velocity of 0.5 m/s (40 RPM). A thick layer of aqueous inorganic polymer glass lubricant is sprayed on the rolls prior to strip entry into the roll bite. As the length of the sample (200 mm) is appreciably shorter than the circumference of the roll (706.5 mm), the sample can be fully lubricated during the whole rolling process. After rolling, the rolled samples were immediately put into a sealed box and purged with nitrogen gas to eliminate the secondary oxidation. The rolling process is schematically illustrated in Figure 2.

**Figure 2.** Schematic of the hot rolling experiments.

2.3. Characterizations

Phase constituents of NSO were identified by X-ray Diffractometer (GBC MMA) with $\text{Cu-K}\alpha$ radiation source. The set step size and scan speed are 0.02° and $1^\circ/\text{min}$, respectively.

The surface profile of the rolled surface was observed by the 3-D profile (Bruker, Billerica, MA, USA). Morphologies and chemical composition of the rolled sample surface of the counterparts were examined by a JSM-6490LV scanning electron microscopy (SEM) attached with energy dispersive spectroscopy (EDS).

3. Result and discussion

3.1. Hot Rolling Results for Un-Descaled Conditions

The hot rolling results under the lubrication of different concentrations of NSO for un-descaled strips are given in Figure 3. As can be seen in Figure 3a, the rolling force under water lubrication is around 230 kN. When the NSO is applied, the rolling force is reduced by 7.8% compared to the water-lubricated condition, with the lowest of 212 kN at 18 wt.% concentration, 7.8% reduction compared to the 0 wt.% NSO. The rolling force is at the same level as that of the concentration of 18 wt.%, even under higher concentration.

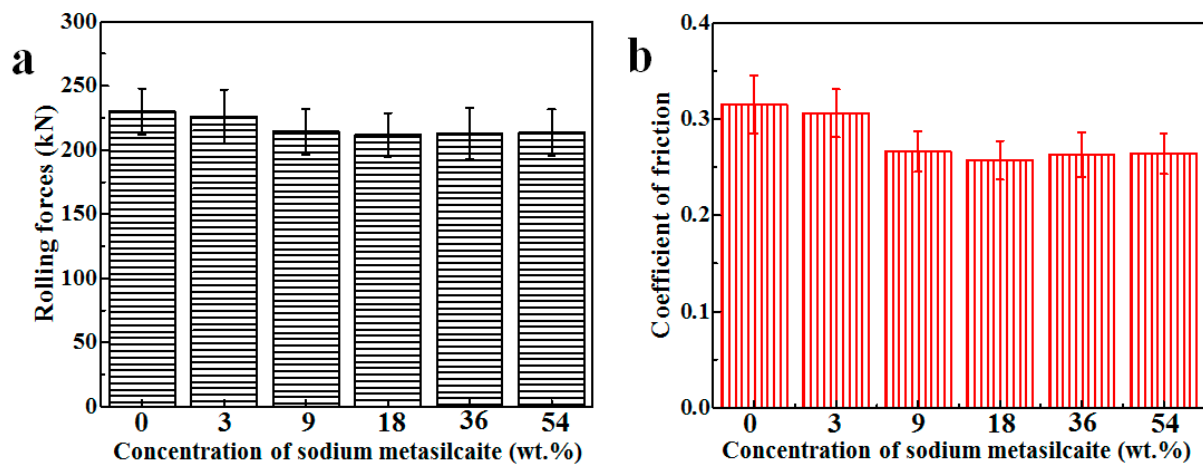


Figure 3. Rolling force (a) and coefficient of friction (b) as a function of the concentration of the NSO for un-descaled strips.

The coefficient of friction is calculated by an inverse method according to the Alexander Model [48]. The results are shown in Figure 3b. It can be seen that the calculated coefficient of friction shows the same trend as the rolling force, where the coefficient of friction was reduced for the NSO applied condition, with the value decreased from 0.315 for the water lubricated condition to 0.257 with 18 wt.% NSO lubrication. Thus, the results above suggest that the sodium metasilicate is an effective lubricant for the hot rolling process, and the optimal concentration was 18 wt.%. The reverse calculation of the coefficient of friction based on Equations (1)–(5)

$$P = B \cdot K \cdot \sqrt{R1 \cdot \Delta h} \cdot \left(1.08 + 1.79 \cdot \mu \cdot r \cdot \sqrt{\frac{R}{h1}} - 1.02 \cdot r \right) \cdot \left(1 - \frac{C \cdot t1 + (1 - c)t2}{K} \right) \quad (1)$$

where P and μ are the rolling force and coefficient of friction, B , $R1$, Δh , C , $t1$, and $t2$ are the stripe width, radius of the deformed work roll, rolling reduction, coefficient, and front and back tension stress. The radius of the deformed roll $R1$ was calculated based on the equation:

$$R1 = R \cdot \left[1 + \frac{16(1 - v^2)P}{\pi E \Delta h} \right] \quad (2)$$

According to [49], the yield stress of steel is:

$$\sigma = \sigma_0 \times e^{-aT} \times b1 \epsilon^{m1} \times b2 \dot{\epsilon}^{m2} \quad (3)$$

where σ and σ_0 are the yield stress and base yield stress, ϵ , $\dot{\epsilon}$, and T are the strain, strain rate (s^{-1}), and temperature (K), respectively. A , b_1 , b_2 , m_1 and m_2 are all constants. In Alexander's program, the flow stress is modified as:

$$Y = A \times \text{Exp}(BT) \times (1 + C\epsilon)^{n_1} \times (1 + D\dot{\epsilon})^{n_2} \quad (4)$$

where A , B , C , D , n_1 , and n_2 are constant for mild steel, and the determined results are shown below:

$$Y = 158.44 \times \text{Exp}(-002532T) \times (1 + 1000\epsilon)^{0.3695} \times (1 + 1000\dot{\epsilon})^{0.1097} \quad (5)$$

It can be seen that the calculated coefficient of friction and the torque show the same trend with that of the rolling force, where the coefficient of friction and torque also reduced for the NSO added conditions, with the value decrease from 0.26 and 5.6 kN·m for the pure water lubricated condition to 0.21 and 5.3 kN·m. Thus, the results above suggest that the NSO has the lubrication effect for the hot rolling, and the optimal concentration for the sodium metasilicate is 18 wt.%.

3.2. Surface Observation of Rolled Strips under Un-Descaled Condition

As the surface quality of the hot rolled strips is an important parameter, the 3D profile and roughness results are shown in Figure 4. After oxidation at high temperatures, the roughness is increased due to oxidation at high temperature. The surface roughness of the strip surface under 0 wt.% NSO lubrication is about 4.95 μm . It is slightly reduced to 2.83 μm for 18 wt.% NSO adding condition, while slight decreases are observed with the increase in concentration of NSO. The lubricant could fill into the cracks on the oxide scale and partially prevent the direct roll/strip contact to reduce the roughness. However, the non-continuous tribofilm might increase the roughness, leading to a slightly reduced surface roughness.

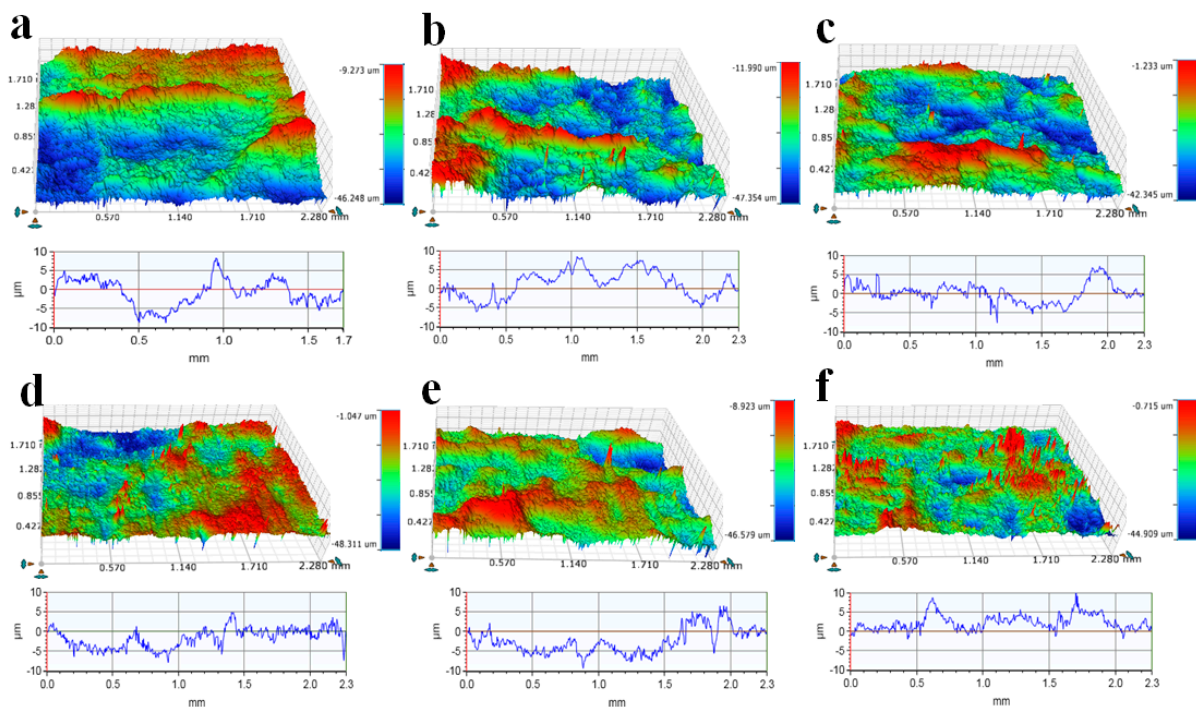


Figure 4. 3D and 2D profilometer images of the rolled samples surface under different concentrations of sodium metasilicate; (a) 0 wt.%, (b) 3 wt.%, (c) 9 wt.%, (d) 18 wt.%, (e) 36 wt.%, (f) 54 wt.%.

As the original roughness of the roller is only around 1 μm , the applied load on the hot strips compresses the oxide scale, producing spalling and some cracks. In Figure 5,

spalling and grooves result from scratches of asperities. The oxide scale is observed for the water-lubricated condition at a higher NSO concentration of 18 wt.% (Figure 5d), negligible grooves are observed, and some adhered films are found. EDS mapping of the representative film (marked red box region shown in Figure 5f) is present in Figure 6. The films are rich in Na, EDX spectrum of spots B and C, and the relative composition is shown in Figure 6b,c. The smooth region of spot C contained more Na and O, indicating the existence of lubricant on the surface of hot rolled strips. It is clear that the Mn is rich on the worn surface, which is consistent with our previous ball-on-disc test that Mn aggregated to the top surface in the metasilicate glass lubricated conditions [33].

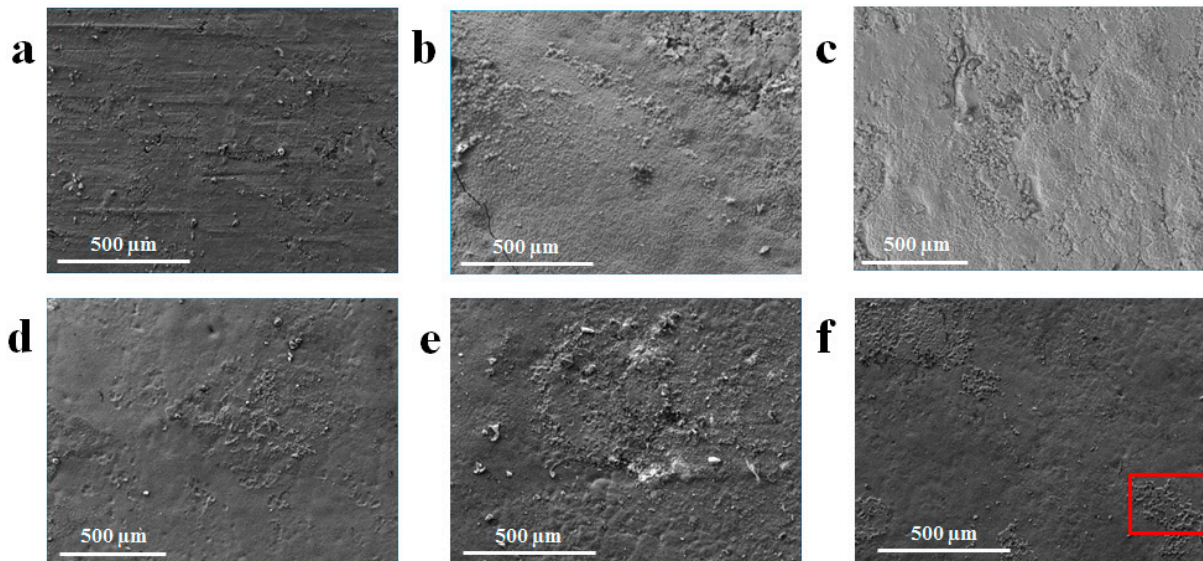


Figure 5. Secondary electron images of the rolled sample surface under different concentration of NSO; (a) 0 wt.%, (b) 3 wt.%, (c) 9 wt.%, (d) 18 wt.%, (e) 36 wt.%, (f) 54 wt.%.

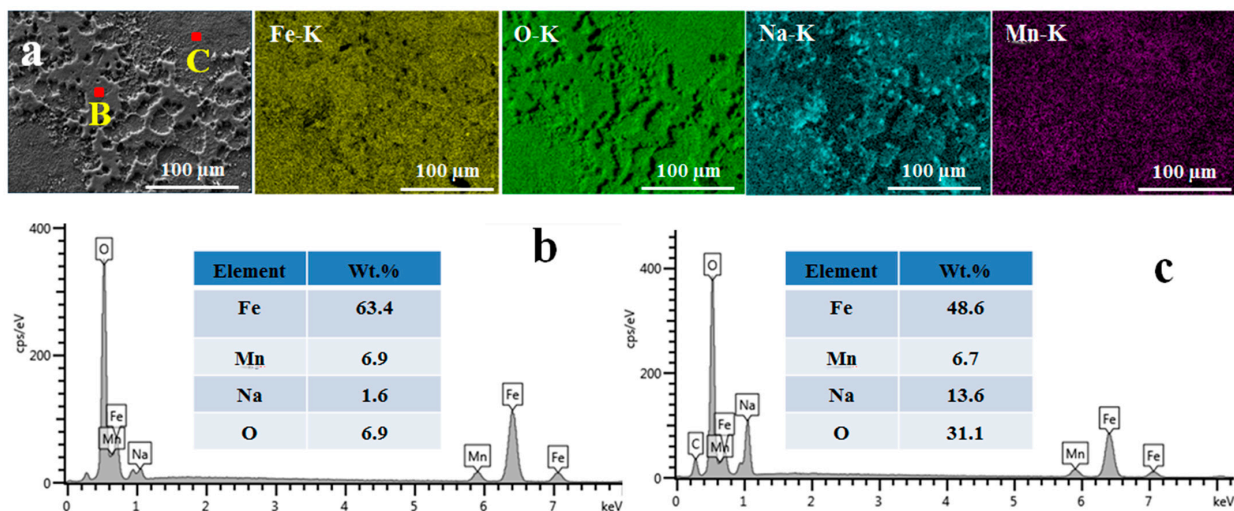


Figure 6. SEI of the marked red square region in Figure 5 and the corresponding EDS mapping and EDX spectra.

The morphology of the cross-section and the corresponding elemental distribution are shown in Figure 7. For different concentrations of NSO, the oxide scale thickness is about 50 μm with the NSO-lubricated condition, compared to 70 μm with the water-lubricated condition. For the concentration below 9 wt.%, negligible Na and Si were observed. At 18 wt.% and above, large amounts of Na and Si are detected in the oxide scale and the strip surface. Some of the NSO were compressed into the oxide scale; thus, the Na and Si can

also be found in the oxide scale and fill the cracks. These Na and Si are also likely to hinder the inward diffusion of oxygen and reduce oxidation as a result.

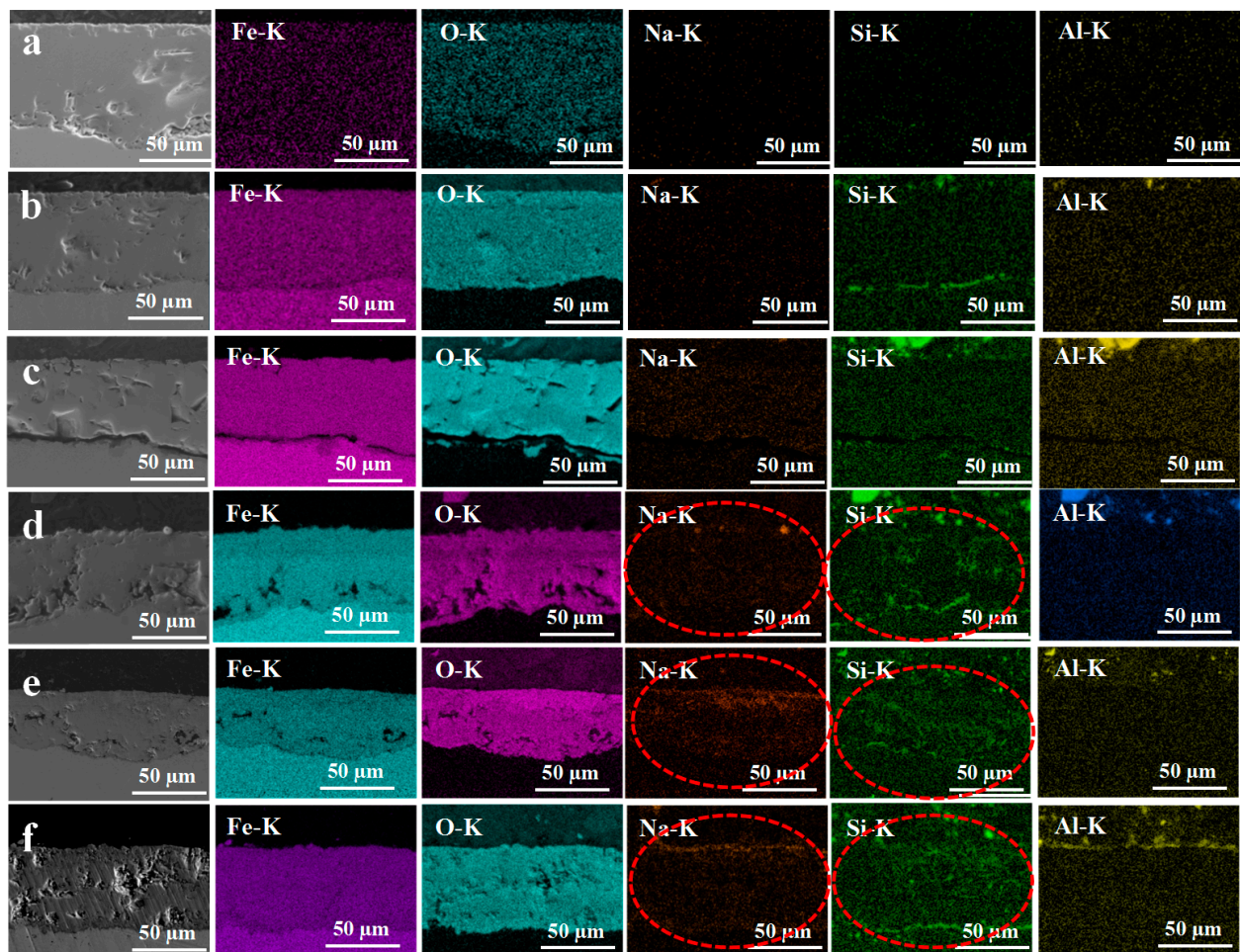


Figure 7. SEIs of the cross section of the rolled samples and their corresponding EDS mappings; (a) 0 wt.%, (b) 3 wt.%, (c) 9 wt.%, (d) 18 wt.%, (e) 36 wt.%, (f) 54 wt.%.

3.3. Hot Rolling Results for Descaled Conditions

To further identify the influence of the oxide scale on the lubricating effects of NSO, hot rolling tests were also conducted for the descaled strips. As can be seen in Figure 8, the rolling force and reverse calculated coefficient of friction show a decreasing trend with the increase in NSO concentration. It is 245 kN for the water lubrication, a 12.7% reduction to 214 kN at 18 wt.%, and a minor decrease with the increase in NSO concentration. In Figure 8b, the reversed calculated coefficient of friction is 0.335 for the 0 wt.% NSO condition, and reduced to 0.267 when the concentration of NSO is 18%, it keeps this level with further increasing of NSO concentration. Compared to the 7.8% reduction for the undescalded condition shown in Figure 3, the reduction in rolling force for the descaled strips is larger, indicating a better lubricating effect of NSO for the descaled strips, which means that the existence of oxide scale will deteriorate the lubricating effects.

3.4. Surface Observation of Rolled Strips under Descaled Condition

The rolled surface for the descaled sample was lubricated by 18 wt.% NSO seems more smooth than the sample of 0 wt.% NSO, as shown in Figure 9a,c. In Figure 9c, some small black drops are observed on the sample surface; the elemental distribution shown in Figure 9d indicates the existence of some Na and Si. A higher magnification image of the marked red box in Figure 9c was also shown in Figure 10. It is clear to find some black

drops on the rolled sample surface; EDS mapping in Figure 10b shows strong signals of Na and Si at the black drops region, suggesting the aggregation of the melted NSO. EDX spectrum of the marked red spots (C and D) are illustrated in Figure 10c,d; compared with the strong signal of Na and Si in spot C, a small amount of Na and Si are observed on the non-melt covered region.

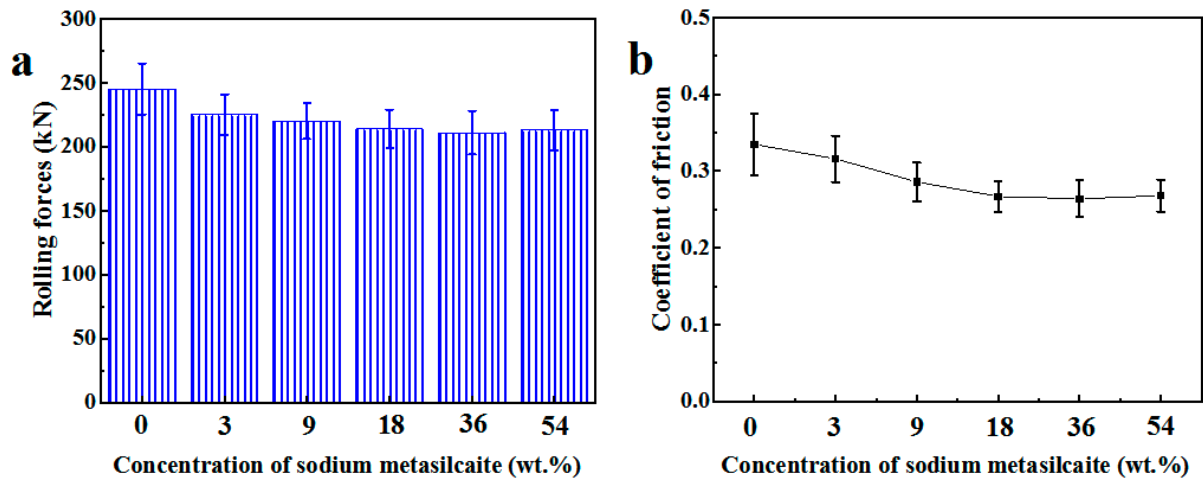


Figure 8. Rolling force (a) and coefficient of friction (b) as a function of the concentration of the NSO for the oxide scale descaled condition.

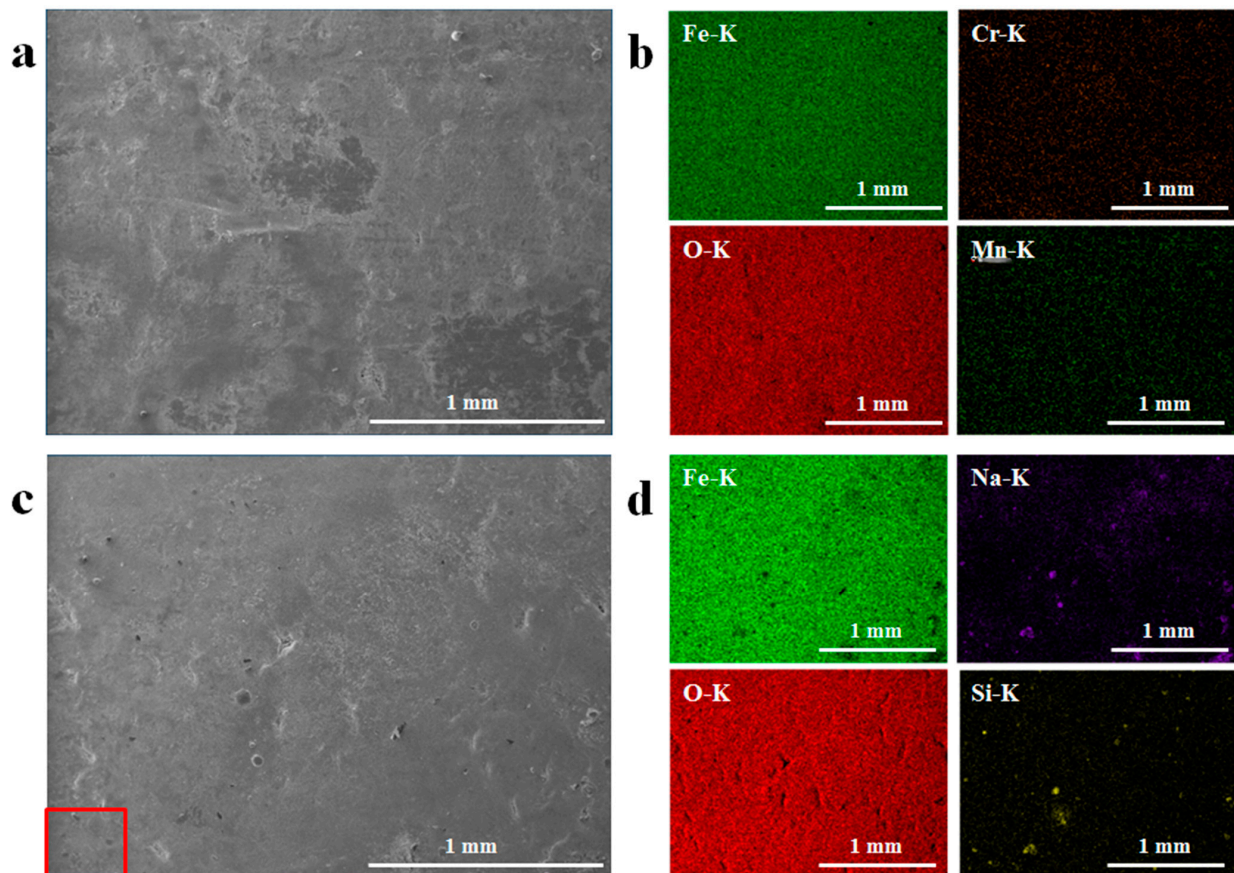


Figure 9. SEM images and corresponding EDS mapping of the rolled surface for 0 wt.% NSO samples (a,b) and samples under 18 wt.% NSO (c,d).

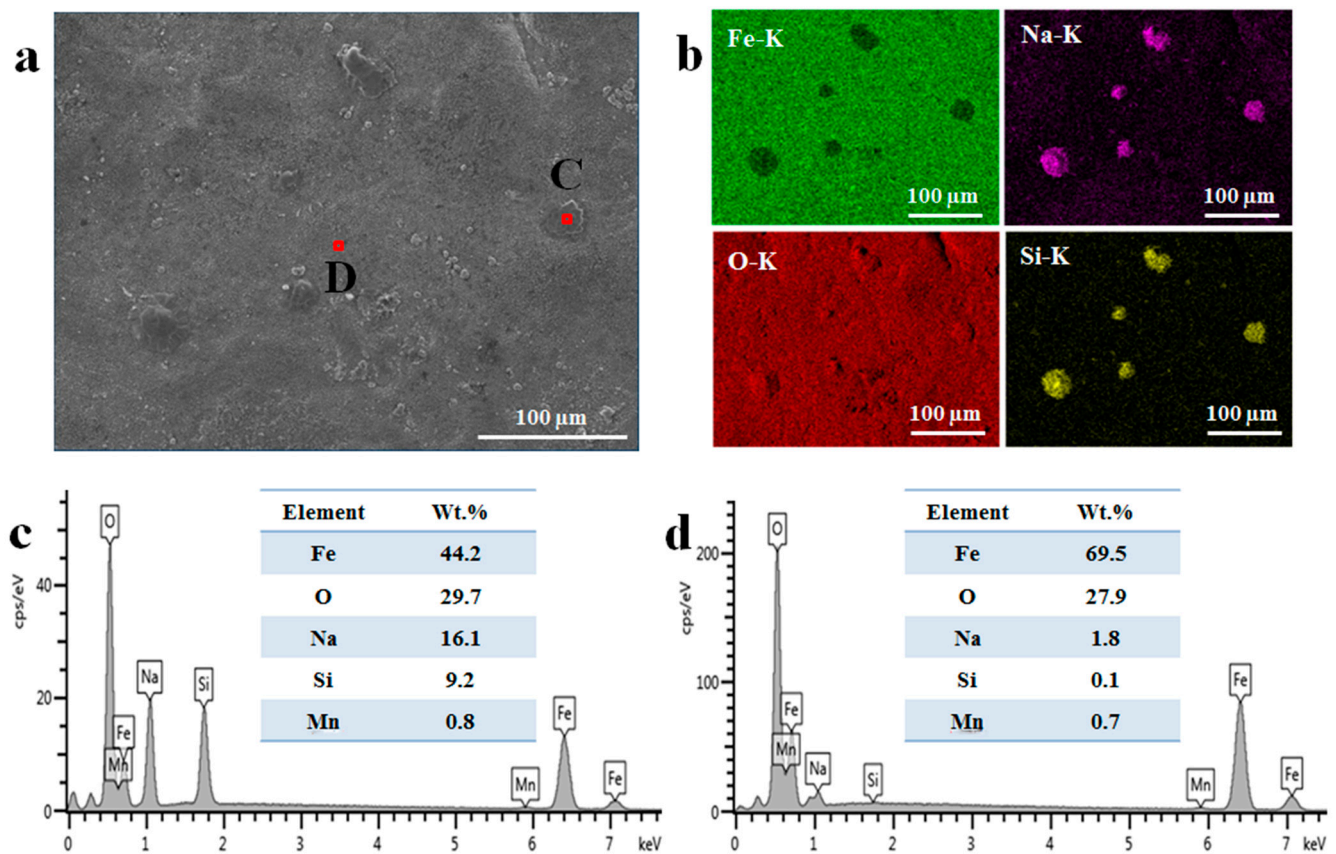


Figure 10. SEIs of the cross-section of the rolled samples and their corresponding EDS mappings; (a) SEM image of the red box marked region in Figure 9c, (b) the corresponding EDS mappings, the spectrum of marked spot (c) C and (d) D in Figure 10a.

The lubrication effect of NSO is concentration-dependent; the optimal results are obtained when it is 18 wt.% and above. Further increase in the NSO did not further reduce the rolling force. It is likely due to the fact that when the concentration of NSO is 18 wt.%, the NSO can almost cover the sample surface, further increases in the content, can only slightly increase the thickness of the NSO layer, and have a slight influence on the frictional results. When the concentration is below 18 wt.%, the NSO is not enough for the coverage of the samples, leading to a partial separation of the roller and strips and thus showing poorer lubrication effects. After rolling, the NSO does not appear to cover the strips; this results from the fact that some NSO is compacted into the oxide scale, and the strips are enlarged after hot deforming. The descaling process and the oxide scale can influence the rolling and friction results. For the un-descaled hot strips, a thick oxide scale (hundred micrometers) forms on the strip; it is even tens of micrometers after rolling. As can be seen in Figure 7, it is about 70 μm . Compared with the dense substrate, the oxide scale is normally softer with large amounts of voids; high pressure during rolling will also break the oxide scale and cause cracks. NSO will be compacted, sheared, and mixed with the soft oxide scale during the rolling process, thus weakening the lubrication effect to some extent, as illustrated in Figure 11.

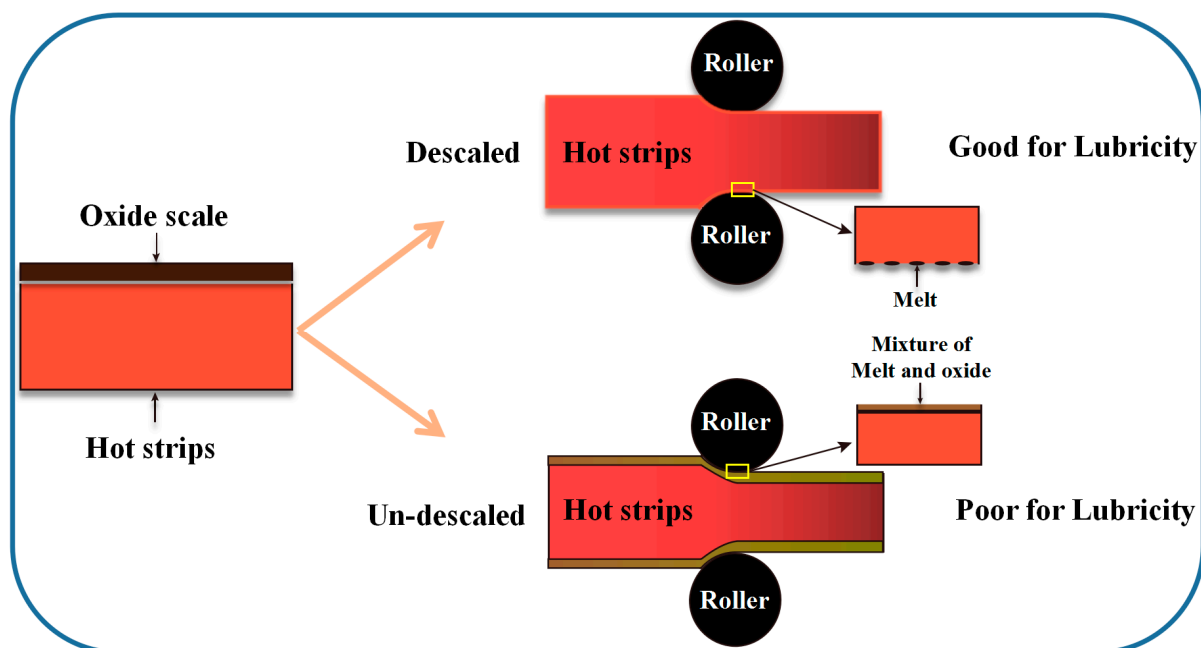


Figure 11. Mechanism for lubrication difference of NSO under descaling and un-descaling conditions.

The hot rolling results suggest that NSO can function as a lubricant for the hot metal forming process. However, the efficiency differs from that of the laboratory ball-on-disc results reported previously [50,51]. The laboratory ball-on-disc results indicate that the NSO has promising lubrication effects at 920 °C and above due to the glass transition and pre-melting of NSO. The formed glass with low viscosity can offer an easy sliding interface, thus reducing friction and wear. The reduction in the coefficient of friction can reach 50%, much higher than the hot rolling process. This results from the difference in working conditions and configuration between the hot rolling experiment and ball-on-disc tests. Firstly, the NSO is coated on the discs and heated to the target temperature to perform tests, and the tests last for 15 min, which means the long-time exposure of NSO at high temperature and frictional heat produced during continuous sliding can ensure its transformation from solid state to the melt and provide lubrication [50]. For the hot rolling process, the duration of the contacts of the roller and hot strip is only $10^{-2}\sim 10^{-3}$ s; the lubricant is sprayed on the hot roller, considering the diameter of the roller (706.86 mm), the 200 mm length strips can be lubricated within one revolution. Some NSO particles are unlikely to be fully transformed into a viscous liquid to offer lubrication. When the lubricant is coated on the discs for the ball-on-disc test, the water is evaporated at high temperatures while it is sprayed on the cold roller in the hot rolling process. The existence of oxide scale is also believed to weaken the lubrication effect of the NSO glass lubricant, as the iron oxide scale formed on the steel surface is generally loose, some of the NSO glass is likely to be compacted, sheared, and even mixed with the soft oxide scale through the holes and cracks during the high deformation process.

For the descaled tests, the NSO easily forms the easily sheared melt at the rolling interface. Therefore, it is important for the descaling process to control the oxide scale. During the descaling process, the descaling time must be kept constant to exclude the influence of the temperature differentials, which is vital in the hot rolling process.

4. Conclusions

This paper deals with the lubrication effects of pure sodium metasilicate. The influence of the concentration of NSO and descaling on the rolling force and the inverse calculated coefficient of friction was studied. The rolled surface morphology and elemental distribution were characterized. The key findings of this work are:

- (1) The lubrication effect of sodium metasilicate was concentration and descaling dependent; when the concentration of NSO is 18 wt.% and above, the optimal lubricating effect is obtained. It results from the coverage difference of NSO on the strip surface.
- (2) Descaling that removing the oxide scale can influence the lubricating effects. The dense strips exposed after descaling will provide a substrate for the melt NSO and offer a hard-soft interface for easy shearing; thus, the destructive abrasive wear is reduced, contributing to a smooth surface and a significant reduction in friction and wear.
- (3) For the un-descaling conditions, the NSO will be compacted and mixed with the oxide scale, and thus weaken the lubricating effect in some effect.

Author Contributions: Methodology, X.W.; Investigation, J.H., X.S. and P.W.; Writing—original draft, H.L.; Supervision, G.D. and L.W. All authors have read and agreed to the published version of the manuscript.

Funding: This work was funded by the National Natural Science Foundation of China (No. 52205215) and the Fundamental Research Funds for the Central Universities (No. G2022KY05105).

Data Availability Statement: Data sharing does not apply to this article.

Conflicts of Interest: The authors declare no conflict of interest.

References

1. Dohda, K.; Boher, C.; Rezai-Aria, F.; Mahayotsanun, N. Tribology in metal forming at elevated temperatures. *Friction* **2015**, *3*, 1–27. [[CrossRef](#)]
2. Wang, L.; Geng, Y.; Tieu, A.K.; Hai, G.; Tan, H.; Chen, J.; Yang, J. In-situ formed graphene providing lubricity for the FeCoCrNiAl based composite containing graphite nanoplate. *Compos. Part B Eng.* **2021**, *221*, 109032. [[CrossRef](#)]
3. Zhang, H.; Le, K.; Wang, C.; Sun, J.; Xu, S.; Liu, W. Influence of Deposition Temperature on the Structure and Current-Carrying Friction Performance of Cu Films by DC Magnetron Sputtering Technology. *Lubricants* **2022**, *11*, 8. [[CrossRef](#)]
4. Geng, Y.; Chen, W.; Tan, H.; Cheng, J.; Zhu, S.; Yang, J.; Liu, W. Remarkable Wear Resistance in a Complex Concentrated Alloy with Nanohierarchical Architecture and Composition Undulation. *Research* **2023**, *6*, 0160. [[CrossRef](#)]
5. Nguyen, C.; Tieu, A.K.; Deng, G.; Wexler, D.; Vo, T.D.; Wang, L.; Yang, J. Tribological performance of a cost-effective CrFeNiAl_{0.3}Ti_{0.3} high entropy alloy based self-lubricating composite in a wide temperature range. *Tribol. Int.* **2022**, *174*, 107743. [[CrossRef](#)]
6. Zhen, J.; Han, Y.; Cheng, J.; Chen, W.; Yang, J.; Jia, Z.; Zhang, R. Enhancing the wide temperature dry sliding tribological performance of nickel-alloy by adding MoS₂/CaF₂. *Tribol. Int.* **2022**, *165*, 107254. [[CrossRef](#)]
7. Beynon, J. Tribology of hot metal forming. *Tribol. Int.* **1998**, *31*, 73–77. [[CrossRef](#)]
8. Chun, Y.-D.; Lee, J.; Lee, J.; Suh, J. Thermal preload for predicting performance change due to pad thermal deformation of tilting pad journal bearing. *Lubricants* **2022**, *11*, 3. [[CrossRef](#)]
9. Cui, S.; Liu, Y.; Wang, T.; Tieu, K.; Wang, L.; Zeng, D.; Li, Z.; Li, W. Tribological behavior comparisons of high chromium stainless and mild steels against high-speed steel and ceramics at high temperatures. *Friction* **2022**, *10*, 436–453. [[CrossRef](#)]
10. Huang, S.; Wu, H.; Jiang, Z.; Huang, H. Water-based nanosuspensions: Formulation, tribological property, lubrication mechanism, and applications. *J. Manuf. Process.* **2021**, *71*, 625–644. [[CrossRef](#)]
11. Wang, L.; Tieu, A.K.; Wang, J.; Sang, P.T.; Xia, C.; Zhu, H.; Deng, G. High load capability, sticking scale inhabitation and promising lubrication of sodium carbonate coating for steel/steel contact at high temperature. *Tribol. Int.* **2021**, *153*, 106594. [[CrossRef](#)]
12. Deng, G.; Tieu, A.K.; Su, L.; Wang, P.; Wang, L.; Lan, X.; Cui, S.; Zhu, H. Investigation into reciprocating dry sliding friction and wear properties of bulk CoCrFeNiMo high entropy alloys fabricated by spark plasma sintering and subsequent cold rolling processes: Role of Mo element concentration. *Wear* **2020**, *460–461*, 203440. [[CrossRef](#)]
13. Wang, W.; Wei, P.; Liu, H.; Zhu, C.; Deng, G.; Liu, H. A micromechanics-based machine learning model for evaluating the microstructure-dependent rolling contact fatigue performance of a martensitic steel. *Int. J. Mech. Sci.* **2023**, *237*, 107784. [[CrossRef](#)]
14. Cheng, J.; Zhu, S.; Tan, H.; Wang, S.; Sun, Q.; Ding, Y.; Yang, J. High temperature tribological behaviors of MoAlB ceramic from 800–1200 °C. *Tribol. Int.* **2023**, *185*, 108522.
15. Schell, L.; Emele, M.; Holzbeck, A.; Groche, P. Investigation of different lubricant classes for aluminium warm and hot forming based on a strip drawing test. *Tribol. Int.* **2022**, *168*, 107449. [[CrossRef](#)]
16. Astakhov, V.P. Tribology of metal cutting. In *Mechanical Tribology*; Marcel Dekker: New York, NY, USA, 2004; pp. 307–346.
17. Tieu, A.; Kosasih, P.B.; Godbole, A. A thermal analysis of strip-rolling in mixed-film lubrication with O/W emulsions. *Tribol. Int.* **2006**, *39*, 1591–1600. [[CrossRef](#)]

18. Edla, S.; Thampi, A.D.; Prasannakumar, P.; Rani, S. Evaluation of physicochemical, tribological and oxidative stability properties of chemically modified rice bran and karanja oils as viable lubricant base stocks for industrial applications. *Tribol. Int.* **2022**, *173*, 107631. [[CrossRef](#)]
19. Valigi, M.C.; Malvezzi, M.; Logozzo, S. A numerical procedure based on Orowan's theory for predicting the behavior of the cold rolling mill process in full film lubrication. *Lubricants* **2020**, *8*, 2. [[CrossRef](#)]
20. Moshkovich, A.; Perfilyev, V.; Rapoport, L. Effect of Plastic Deformation and Damage Development during Friction of fcc Metals in the Conditions of Boundary Lubrication. *Lubricants* **2019**, *7*, 45. [[CrossRef](#)]
21. Wu, C.; Zhang, L.; Qu, P.; Li, S.; Jiang, Z. A multi-field analysis of hydrodynamic lubrication in high speed rolling of metal strips. *Int. J. Mech. Sci.* **2018**, *142–143*, 468–479. [[CrossRef](#)]
22. Xia, W.; Zhao, J.; Wu, H.; Zhao, X.; Zhang, X.; Xu, J.; Jiao, S.; Wang, X.; Zhou, C.; Jiang, Z. Effects of oil-in-water based nanolubricant containing TiO₂ nanoparticles in hot rolling of 304 stainless steel. *J. Mater. Process. Technol.* **2018**, *262*, 149–156. [[CrossRef](#)]
23. Xia, W.; Zhao, J.; Wu, H.; Zhao, X.; Zhang, X.; Xu, J.; Jiao, S.; Jiang, Z. Effects of oil-in-water based nanolubricant containing TiO₂ nanoparticles in hot rolling of 304 stainless steel. *Procedia Eng.* **2017**, *207*, 1385–1390. [[CrossRef](#)]
24. Altan, T.; Tekkaya, A.E. *Sheet Metal Forming: Fundamentals*; ASM International: Almere, The Netherlands, 2012.
25. Cui, S.; Zhu, H.; Wan, S.; Tieu, K.; Tran, B.H.; Wang, L.; Zhu, Q. Effect of loading on the friction and interface microstructure of lubricated steel tribopairs. *Tribol. Int.* **2017**, *116*, 180–191. [[CrossRef](#)]
26. Yaseen, M.; Rawat, S.K.; Shah, N.A.; Kumar, M.; Eldin, S.M. Ternary hybrid nanofluid flow containing gyrotactic microorganisms over three different geometries with Cattaneo–Christov Model. *Mathematics* **2023**, *11*, 1237. [[CrossRef](#)]
27. Yaseen, M.; Rawat, S.K.; Khan, U.; Negi, A.S.; Kumar, M.; Sherif, E.-S.M.; Hassan, A.M.; Pop, I. Inspection of unsteady buoyancy and stagnation point flow incorporated by Ag-TiO₂ hybrid nanoparticles towards a spinning disk with Hall effects. *Case Stud. Therm. Eng.* **2023**, *44*, 102889. [[CrossRef](#)]
28. Wei, P.; Lu, C.; Tieu, K.; Su, L.; Deng, G.; Huang, W. A study on the texture evolution mechanism of nickel single crystal deformed by high pressure torsion. *Mater. Sci. Eng. A.* **2017**, *684*, 239–248. [[CrossRef](#)]
29. Bay, N.; Azushima, A.; Groche, P.; Ishibashi, I.; Merklein, M.; Morishita, M.; Nakamura, T.; Schmid, S.; Yoshida, M. Environmentally benign tribo-systems for metal forming. *CIRP Ann.* **2010**, *59*, 760–780. [[CrossRef](#)]
30. Morishita, M. Tribology in manufacturing processes of automobiles at Toyota. *Proc. ICTMP* **2007**, *1*, 35–48.
31. Xiong, S.; Liang, D.; Wu, H.; Lin, W.; Chen, J.; Zhang, B. Preparation, characterization, tribological and lubrication performances of Eu doped CaWO₄ nanoparticle as anti-wear additive in water-soluble fluid for steel strip during hot rolling. *Appl. Surf. Sci.* **2021**, *539*, 148090. [[CrossRef](#)]
32. Bao, Y.; Sun, J.; Kong, L. Effects of nano-SiO₂ as water-based lubricant additive on surface qualities of strips after hot rolling. *Tribol. Int.* **2017**, *114*, 257–263. [[CrossRef](#)]
33. Shah, F.U.; Glavatskih, S.; Antzutkin, O.N. Boron in tribology: From borates to ionic liquids. *Tribol. Lett.* **2013**, *51*, 281–301. [[CrossRef](#)]
34. Choudhary, R.; Pande, P. Lubrication potential of boron compounds: An overview. *Lubr. Sci.* **2002**, *14*, 211–222. [[CrossRef](#)]
35. Yabuuchi, N.; Yoshida, H.; Komaba, S. Crystal structures and electrode performance of alpha-NaFeO₂ for rechargeable sodium batteries. *Electrochemistry* **2012**, *80*, 716–719. [[CrossRef](#)]
36. Wang, L.; Tieu, A.K.; Zhu, H.; Deng, G.; Cui, S.; Zhu, Q. A study of water-based lubricant with a mixture of polyphosphate and nano-TiO₂ as additives for hot rolling process. *Wear* **2021**, *477*, 203895. [[CrossRef](#)]
37. Cui, S.; Wan, S.; Zhu, Q.; Tieu, A.K.; Zhu, H.; Wang, L.; Cowie, B. Tribochemical behavior of phosphate compounds at an elevated temperature. *J. Phys. Chem. C* **2016**, *120*, 25742–25751. [[CrossRef](#)]
38. Wan, S.; Tieu, A.K.; Zhu, Q.; Zhu, H.; Cui, S.; Mitchell, D.R.; Kong, C.; Cowie, B.; Denman, J.A.; Liu, R. Chemical nature of alkaline polyphosphate boundary film at heated rubbing surfaces. *Sci. Rep.* **2016**, *6*, 26008. [[CrossRef](#)]
39. Wang, L.; Tieu, A.K.; Deng, G.; Wang, J.; Tran, B.H.; Zhu, H.; Yang, J. In-situ interfacial tribochemistry toward eliminating red-scale of silicon steel in friction process. *Tribol. Int.* **2020**, *143*, 106077. [[CrossRef](#)]
40. Kong, N.; Tieu, A.K.; Zhu, Q.; Zhu, H.; Wan, S.; Kong, C. Tribofilms generated from bulk polyphosphate glasses at elevated temperatures. *Wear* **2015**, *330*, 230–238. [[CrossRef](#)]
41. Yue, W.; Wang, C.; Liu, Y.; Huang, H.; Wen, Q.; Liu, J. Study of the regenerated layer on the worn surface of a cylinder liner lubricated by a novel silicate additive in lubricating oil. *Tribol. Trans.* **2010**, *53*, 288–295. [[CrossRef](#)]
42. Nan, F.; Xu, Y.; Xu, B.; Gao, F.; Wu, Y.; Li, Z. Tribological behaviors and wear mechanisms of ultrafine magnesium aluminum silicate powders as lubricant additive. *Tribol. Int.* **2015**, *81*, 199–208. [[CrossRef](#)]
43. Gao, K.; Chang, Q.; Wang, B.; Zhou, N.; Qing, T. The tribological performances of modified magnesium silicate hydroxide as lubricant additive. *Tribol. Int.* **2018**, *121*, 64–70. [[CrossRef](#)]
44. Singh, D.; Thakre, G.; Konathala, L.; Prasad, V. Friction reduction capabilities of silicate compounds used in an engine lubricant on worn surfaces. *Adv. Tribol.* **2016**, *2016*, 1901493. [[CrossRef](#)]
45. Yu, H.; Xu, Y.; Shi, P.; Wang, H.; Wei, M.; Zhao, K.; Xu, B. Microstructure, mechanical properties and tribological behavior of tribofilm generated from natural serpentine mineral powders as lubricant additive. *Wear* **2013**, *297*, 802–810. [[CrossRef](#)]
46. Bass, J.L.; McDonald, M.J.; Urquhart, J.C. Lubricating Method for Silicate Drilling Fluids. US Patent 6,642,183, 4 November 2003.

47. Matsumoto, K.; Izawa, M.; Nakanishi, T.; Tsubouchi, K. Tribological properties of water glass lubricant for hot metalworking. *Tribol. Trans.* **2009**, *52*, 553–559. [[CrossRef](#)]
48. Alexander, J.M. On the theory of rolling. *Proc. R. Soc. Lond. A Math. Phys. Sci.* **1972**, *326*, 535–563.
49. Pietrzyk, M.; Cser, L.; Lenard, J. *Mathematical and Physical Simulation of the Properties of Hot Rolled Products*; Elsevier: Amsterdam, The Netherlands, 1999.
50. Wang, L.; Tieu, A.K.; Cui, S.; Deng, G.; Wang, P.; Zhu, H.; Yang, J. Lubrication mechanism of sodium metasilicate at elevated temperatures through tribo-interface observation. *Tribol. Int.* **2020**, *142*, 105972. [[CrossRef](#)]
51. Wang, L.; Tieu, A.K.; Zhu, H.; Deng, G.; Hai, G.; Wang, J.; Yang, J. The effect of expanded graphite with sodium metasilicate as lubricant at high temperature. *Carbon* **2020**, *159*, 345–356. [[CrossRef](#)]

Disclaimer/Publisher's Note: The statements, opinions and data contained in all publications are solely those of the individual author(s) and contributor(s) and not of MDPI and/or the editor(s). MDPI and/or the editor(s) disclaim responsibility for any injury to people or property resulting from any ideas, methods, instructions or products referred to in the content.